sciendo

POLISH MARITIME RESEARCH 2 (106) 2020 Vol. 27; pp. 76-84
10.2478/pomr-2020-0029

DESIGN AND EXPERIMENT OF LOW-PRESSURE GAS SUPPLY SYSTEM FOR DUAL FUEL ENGINE

Xiaoyong Gu[1]
Guohe Jiang[1]
Zhenghua Guo[2]
Shangzhi Ding[2]
[1] Shanghai Maritime University, China
[2] Shanghai Marine Equipment Research Institute, China

ABSTRACT

A low-pressure gas supply system for dual fuel engines was designed to transport liquid natural gas from a storage tank to a dual fuel engine and gasify it during transportation. The heat exchange area and pressure drop in the spiral- wound heat exchanger, the volume of the buffer tank and the pressure drop in the pipeline of the gas supply system were calculated by programming using Python. Experiments were carried out during the process of starting and running the dual fuel engine using this gas supply system. Experimental data show that the gas supply system can supply gas stably during the process and ensure the stable operation of the dual fuel engine. The effects of the parameters of natural gas and ethylene glycol solution on the heat exchange area of the spiral-wound heat exchanger and the volume of the buffer tank in the gas supply system were studied. The results show that the heat exchange area calculated according to pure methane can adapt to the case of non-pure methane. The temperature difference between natural gas and ethylene glycol solution should be increased in order to reduce the heat exchange area. The heat exchange area selected according to the high pressure of natural gas can adapt to the low pressure of natural gas. The volume of the buffer tank should be selected according to the situation of the minimum methane content to adapt to the situation of high methane content. The main influencing factor in selecting the volume of the buffer tank is the natural gas flow. The results can provide guidance for the design of the gas supply system for dual fuel engines.

Keywords: gas supply system, dual fuel engine, spiral-wound heat exchanger, buffer tank

INTRODUCTION

As a reliable fuel, diesel-oil has been used widely in large ships. However, SO_2 and NO_X released by diesel combustion are harmful to human beings and pollute the environment [1]. In order to control the emission of SO_2, many countries [2, 3] have tested and analysed the amount of SO_2 in air. If the amount of NO_X and hydrocarbons in the atmosphere reaches a certain value under ultraviolet radiation, photochemical reactions will be caused, and finally photochemical smog will be formed. Photochemical smog is very harmful to human beings [4].

In order to reduce the amount of air pollutants from ships, the International Maritime Organization (IMO) has proposed that the sulphur content in ship fuel should be less than 0.5% from January 1, 2020 [5]. The NO_X emission of a ship engine with a speed of 1000 rpm should be less than 2.25 g/(kW·h) [6].

Using natural gas instead of diesel is an important way to reduce the emission of air pollutants. Dual fuel engines are used to enable natural gas to provide power to ships. The operation mode of the dual fuel engine is divided into oil mode and gas mode.

NOMENCLATURE

A	– heat exchange area (m^2)
D	– shell side fluid equivalent diameter (m)
d	– piping diameter (m)
d_o	– piping outside diameter (m)
Gr	– Grashof number
g	– gravitational acceleration (m/s^2)
h	– heat transfer coefficient ($W/m^2/K$)
h_{in}	– enthalpy of inlet natural gas (J/kg)
h_{out}	– enthalpy of outlet natural gas (J/kg)
$i_{l\text{-}g}$	– latent heat of vaporisation (J/kg)
K	– total heat transfer coefficient ($W/m^2/K$)
Nu	– Nusselt number
Pr	– Prandtl number
Δp	– pressure drop (MPa)
ΔQ	– heat exchange (W)
q_m	– mass flow intensity of natural gas (kg/s)
R	– gas constant (J/mol/K)
R_i	– fouling thermal resistance in pipe (K/W)
R_o	– fouling thermal resistance out of pipe (K/W)
Re	– Reynolds number
T_1	– inlet temperature of ethylene glycol aqueous solution (K)
T_2	– outlet temperature of ethylene glycol aqueous solution (K)
t_1	– inlet temperature of natural gas (K)
t_2	– outlet temperature of natural gas (K)
u	– velocity (m/s)
V_m	– volume (m^3)
W_g	– mass flow of natural gas (kg/s)
W_l	– mass flow of liquid natural gas (kg/s)
x	– quality
α	– coefficient of thermal expansion (K-1)
λ	– thermal conductivity (W/m/K)
λ_f	– resistance coefficient
ρ_g	– density of natural gas (kg/m^3)
ρ_l	– density of liquid natural gas (kg/m^3)
μ_g	– dynamic viscosity of natural gas (Pa·s)
μ_l	– dynamic viscosity of liquid natural gas (Pa·s)
μ_f	– dynamic viscosity at flow temperature (Pa·s)
μ_w	– dynamic viscosity at wall temperature (Pa·s)
ν	– kinematic viscosity (m^2/s)
ζ	– coefficient of local resistance

In the oil mode, diesel is used and natural gas is not used. In the gas mode, natural gas is used mainly, and a small amount of diesel is used to ignite the natural gas. There are almost no SO_2 emissions due to the low sulphur content of natural gas. In addition, the emission of SO_2 from the combustion of diesel is very small relative to the total emission. In general, the emission of SO_2 in the gas mode of a dual fuel engine is much lower than that of a diesel engine. Dual fuel engines also emit less nitrogen oxide than diesel engines [7, 8].In order to facilitate storage and transportation, natural gas is usually liquefied and stored in tanks at a certain pressure and gasified when needed. A dual fuel engine uses natural gas rather than liquid natural gas, so a gas supply system is needed to heat and gasify the liquid natural gas into gaseous, pressurised, temperature-controlled gas to be burned in dual fuel engines. Gas supply systems typically include gasifiers, buffer tanks, and accessory pipes. In addition, pumps are required in high-pressure gas supply systems to supply gas to two-stroke dual fuel engines [9].

This paper mainly discusses the low-pressure gas supply system as shown in Fig. 1. LNG from the storage tank is gasified and heated to a certain temperature in the gasifier, passing through the buffer tank and entering the GVU. The fluid used to exchange heat with the LNG in the gasifier is ethylene glycol aqueous solution, due to its high specific heat capacity, low risk and non-solidification at 0°C. After cooling with natural gas, the ethylene glycol solution is heated by hot water from the ship's engine and pressurised by pump. There is no pump in the system to pressurise the natural gas due to the fact that the natural gas pressure has been reduced through the gasifier and pipeline. However, it is still higher than the allowable supply pressure of the dual fuel engine. The equipment gasifying the LNG in the system is a heat exchanger. Nowadays the widely used heat exchangers are plate heat exchangers [10], shell heat exchangers [11] and u-tube heat exchangers [12]. Compared with these heat exchangers, spiral-wound heat exchangers have a compact structure, high operating pressure in the tube and high heat exchange efficiency [13]. They have great advantages for ships which have limited equipment space. The spiral-wound heat exchanger is mainly composed of the core tube, spacer, heat transfer tube and shell, and the working substance in it can be methane, ethane, propane, nitrogen, etc., which is used widely in the gasification and heating of natural gas. In addition, as the amount of LNG in the storage tank decreases, the pressure in the storage tank decreases. In order to maintain the stability of the pressure in the storage tank, a small amount of LNG needs to be gasified and transported back to the tank. Therefore, the gasifier is divided into two zones: the LNG gasified in zone 1 is transported to the dual fuel engine, and the LNG gasified in zone 2 is transported back to the storage tank. The spiral-wound heat exchanger is the most important equipment in the whole gas supply system. Selecting a buffer tank with the right volume can help to keep the supply pressure stable when the natural gas flow is increased. Without a buffer tank, the dual fuel engine will switch automatically from gas mode to oil mode when it is loaded.

In this paper, a low-pressure gas supply system is designed. In order to verify the reliability of the designed system, experiments on the start-up and operation of the gas supply system and dual fuel engine are carried out. By changing the composition, mass flow, temperature and pressure of the natural gas and the temperature of the ethylene glycol aqueous solution, the changes of the main components of the gas supply system are obtained, and the problems needing

attention in the design of the gas supply system are made clear. This provides a reference for the design of the gas supply system for the dual fuel engine.

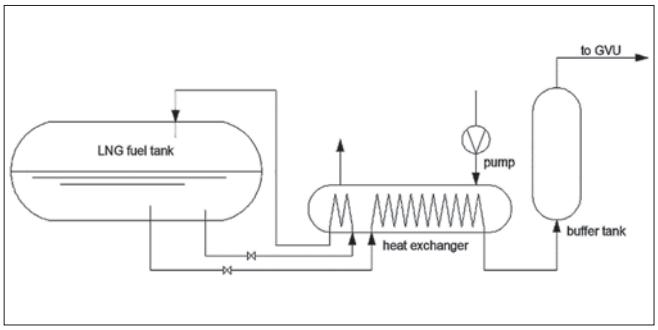

Fig. 1. Low-pressure gas supply system

DESIGN AND EXPERIMENT

DESIGN OF GAS SUPPLY SYSTEM

The gas supply system is mainly composed of the spiral-wound heat exchanger, buffer tank and accessory pipes. The design method is shown below.

The design of the heat exchanger includes the calculation of the heat exchange area and pressure drop.

The heat transfer model formula used in calculation is shown below [14–20]:

$$\Delta Q = q_m(h_{out} - h_{in}) \quad (1)$$

$$A = \Delta Q/(K\Delta t) \quad (2)$$

$$\Delta t = \frac{\Delta t_1 - \Delta t_2}{\ln(\Delta t_1/\Delta t_2)} \quad (3)$$

$$Re = ud/v \quad (4)$$

The saturation boiling heat transfer model provided by Shah is used to determine the heat transfer coefficient in the tube side [21]:

$$G = 4q_m/(\pi d^2) \quad (5)$$

$$Fr_{IO} = G^2/gD\rho^2 \quad (6)$$

$$N = (\frac{1}{x} - 1)^{0.8}(\rho_g/\rho_l)^{0.5} \quad (7)$$

$$h_c = 1.8h_l/N^{0.8} \quad (8)$$

$$h_l = 0.023Re^{0.8}Pr^{0.4}\lambda/d \quad (9)$$

The shell side heat transfer coefficient is determined by the formula provided by Patil [22]:

$$Nu = 0.36Re^{0.55}Pr^{0.33}(\mu/\mu_w)^{0.14} \quad (10)$$

$$\mu/\mu_w = 0.95 \quad (11)$$

$$h_s = \lambda Nu/d \quad (12)$$

The thermal resistances of the tube side, wall and shell side are determined as follows:

$$R_1 = 1/h_l \quad (13)$$

$$R_2 = \ln(\frac{d_o}{d})d/2\lambda_w \quad (14)$$

$$R_3 = d/(d_o h_s) \quad (15)$$

The total heat transfer coefficient is determined as follows:

$$K = \frac{1}{R_1 + R_2 + R_3} + R_1 + d_o R_o/d \quad (16)$$

The frictional pressure drop in the tube is determined by the formula provided by Wang [23]:

$$\Delta p_{lg} = \varphi f G^2 l/(2\rho_l d)c \quad (17)$$

$$c = 1 + x(\frac{\rho_l}{\rho_g} - 1) \quad (18)$$

$$\varphi = (Re\sqrt{\frac{d}{D}})^{0.05} \quad (19)$$

$$f = 0.3164/Re^{0.25} \quad (20)$$

$$\Delta p_{ao} = (\frac{G_l^2}{R_l\rho_l} + \frac{G_g^2}{R_g\rho_g})_o \quad (21)$$

$$\Delta p_{ai} = (\frac{G_l^2}{R_l\rho_l} + \frac{G_g^2}{R_g\rho_g})_i \quad (22)$$

$$\Delta p_t = \Delta p_{lg} + \Delta p_{ao} - \Delta p_{ai} \quad (23)$$

The pressure of natural gas is 0.9 MPa and the corresponding saturation temperature is 144.41 K. Table 1 shows the data used in the calculation.

Tab. 1. Data used in the calculation

Inlet temperature of natural gas (K)	111.15
Outlet temperature of natural gas (K)	283.15
Flow intensity of natural gas (kg/h)	180
Flow of ethylene glycol aqueous solution (m^3/h)	20
Inlet temperature of ethylene glycol aqueous solution (K)	285.45

The result is calculated by programming using Python, and the heat exchange area of the heat exchanger is found to be 3.25 m^2 and the pressure drop in the tube is 1.749 kPa.

In addition to the formulas used to design the heat exchanger, the formulas used to design the buffer tank are as follows:

$$p = \frac{RT}{V_m - b} - \frac{a}{V_m^2} \quad (24)$$

$$Nu_m = 0.48(GrPr)^{1/4} \quad (25)$$

$$Gr = g\alpha\Delta td3/v2 \quad (26)$$

Table 2 shows the data used in the calculation.

Tab. 2. Data used in the calculation

Inlet temperature of natural gas (K)	283.15
Inlet pressure of natural gas (MPa)	0.9
Outlet minimum pressure of natural gas (MPa)	0.85
Maximum flow of natural gas (kg/h)	200
Maximum surge rate	0.5

The result calculated by programming using Python is that the buffer tank volume is 230 dm^3.

The pressure loss in the pipelines transporting LNG is calculated according to the following formulas:

$$\Delta p_{l1} = \lambda_f l \rho v^2 / 2d \tag{27}$$

$$\Delta p_{l2} = \xi \rho v^2 / 2 \tag{28}$$

$$\Delta p_l = \Delta p_{l1} + \Delta p_{l2} \tag{29}$$

Table 3 shows the pipeline parameters and calculation results.

Tab. 3. Pipeline parameters and calculation results

	Length (m)	Diameter (mm)	elbow	Pressure drop(kPa)
Liquid	3	20	4	0.17
Gas	5	25	1	4.8

EXPERIMENT

A dual fuel engine made by Wartsila, model W6L20DF, was used in this experiment. The heat exchanger and dual fuel engine are shown in Fig. 2.

The dual fuel engine was started in oil mode. It was switched to gas mode manually when the load was 350 kW. At this time, the dual fuel engine was fuelled by gas and only a small amount of diesel-oil was injected to ignite the gas. After switching to the gas mode, the load was gradually increased from 350 kW to 900 kW. The dual fuel engine ran for 23 min at the load of 900 kW. Over time, the mass of natural gas in the storage tank decreased and the gas pressure decreased. When the gas pressure was lower than 0.5 MPa, the dual fuel engine switched automatically to oil mode.

DISCUSSION

During the period the load increased from 450 kW to 900 kW. The inlet and outlet temperature of ethylene glycol aqueous solution, as well as the temperature and pressure of natural gas are shown in Fig. 3.

As shown in Fig. 3, the temperature of the gas changes very little in the first 200 seconds, but when the load increases to 750 kW, the gas temperature shows a sudden dropping trend. This is because the residual natural gas in the heat exchangers and buffer tanks before the dual fuel engine start-up had been heated to a certain temperature. The dual fuel engine consumed this gas first. At this time, the flow of natural gas from the storage tank was small because of the small load, and the natural gas was heated to a higher temperature in the heat exchanger. With the passage of time and the increase of load, the residual natural gas was used up, and the flow of natural gas from the storage tank increased greatly. Compared with the residual gas, the temperature of this gas was lower, so the outlet temperature of the gas dropped suddenly. When the load changed, the pressure of the natural gas fluctuated but not greatly.

As the natural gas is consumed in the storage tank, the natural gas pressure decreases. If the pressure of the natural gas decreases to 0.5 MPa, the dual fuel engine will switch to oil mode. When the load is 900 kW, the inlet and outlet temperature of the ethylene glycol aqueous solution, as well as the temperature and pressure of the natural gas are as shown in Fig. 4.

As shown in Fig. 4, with the course of time, the pressure of the natural gas decreased gradually, and the inlet and outlet temperatures of the ethylene glycol aqueous solution

Fig. 2(a). Spiral-wound heat exchanger

Fig. 2(b). Dual fuel engine

were relatively stable. So, the gas supply system can supply gas stably before the dual fuel engine switches to oil mode. The gas temperature increased from 6.3°C to 6.4°C with the decrease of pressure. This is because the specific heat capacity decreased as the pressure decreased. In the process shown in Fig. 4, the inlet and outlet temperatures of the ethylene glycol aqueous solution were constant, so the heat exchange was constant. As the gas pressure decreased, this heat exchange raised the temperature of the natural gas to a higher level.

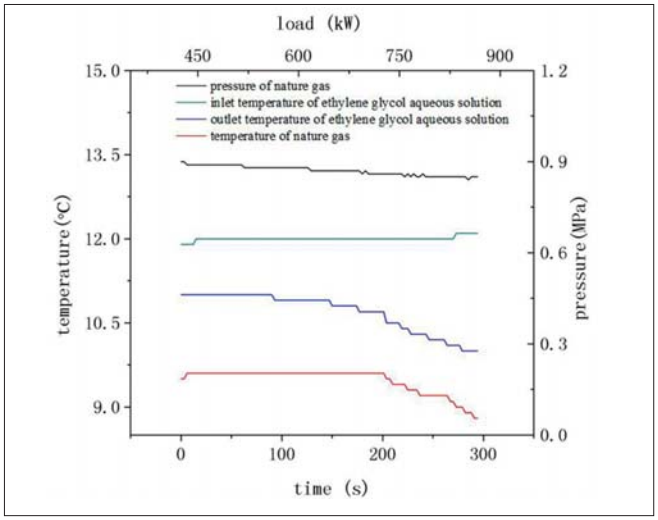

Fig. 3. Parameters change with time

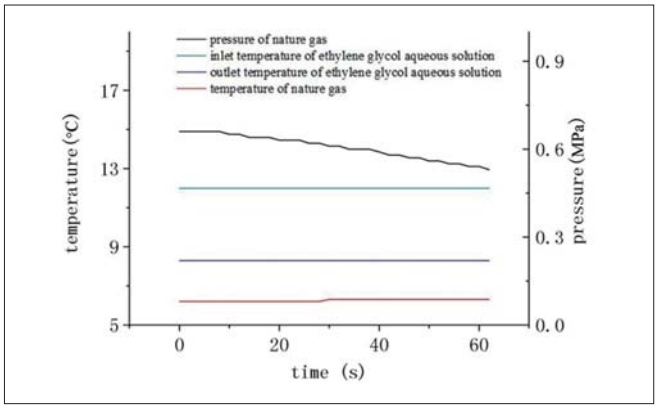

Fig. 4. Parameters changes before switching to oil mode

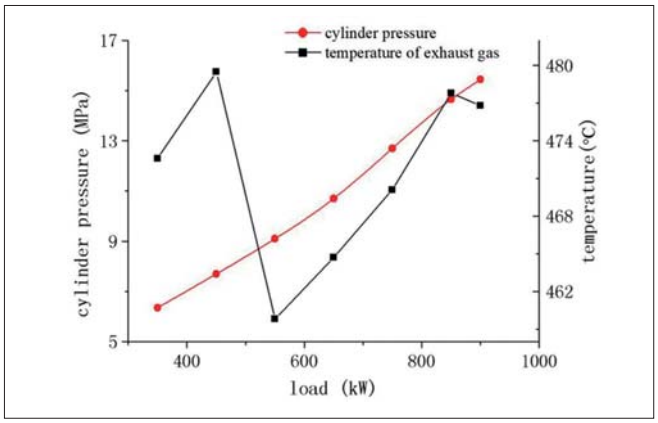

Fig. 5. Cylinder pressure and exhaust temperature vs. engine load

The cylinder pressure and exhaust temperature of the dual fuel engine during the experiment are shown in Fig. 5.

As shown in Fig. 5, the cylinder pressure increased from 6.35 MPa to 15.45 MPa with the increase of load; the highest exhaust temperature was 480°C and the lowest was 460°C, with a variation range of only 4.17%. The dual fuel engine ran stably without stopping or switching to oil mode.

Concluding, the gas supply system can supply gas stably at the start-up and running process of the dual fuel engine.

When designing the gas supply system, the main issue is to design the heat exchange area of the spiral-wound heat exchanger and the volume of the buffer tank. Both these values are affected by the mass flow, temperature and pressure of the natural gas, as well as the temperature of the ethylene glycol solution. Although a heat exchanger having a large heat exchange area and a buffer tank having a large volume can adapt to various conditions, the cost is very high. Therefore, it is necessary to discuss the minimum heat exchange area required for the heat exchanger and the minimum volume required for the buffer tank. These are analysed below.

In order to investigate the applicability of the gas supply system, three variants of natural gas components are selected, and the gas content in each group is shown in Table 4.

Tab. 4. Natural gas components in three groups (%,volume)

Group	methane	ethane	propane	nitrogen	other
1	100	–	–	–	–
2	87.75	3.78	3.74	0.02	4.71
3	77.76	9.74	3.85	1.27	7.38

Group 2 is from Shengli oil field, group 3 is from Pinghu oil and gas field.

With the change of natural gas flow, the change of the heat exchange area of the spiral- wound heat exchanger is shown in Fig. 6.

As shown in Fig. 6, the heat exchange area increases with the increase of the natural gas flow. Due to the increase of the natural gas flow, the amount of heat required per unit of time increases. According to the heat transfer model of the heat exchanger, increasing the heat exchange area can increase the heat exchange per time unit. In addition, different components of natural gas require different heat exchange areas. With the increase of the methane volume fraction, the heat exchange area of the heat exchanger increases. This is because of methane's larger specific heat capacity compared with the other alkanes in natural gas. In order to make the three groups reach the same outlet temperature, a larger heat exchange area is needed by group 1 to obtain enough heat than group 2 and group 3. Therefore, the design of the gas supply process should be based on natural gas with a methane content of 100%.

When the natural gas temperature is lower than the requirement for dual fuel engines, the dual fuel engine will stop or switch automatically to oil mode. In order to ensure that the dual fuel engine runs stably in the gas mode, the outlet

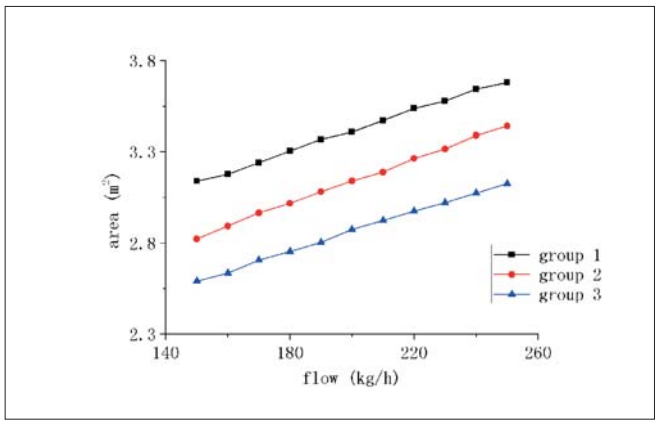

Fig. 6. Heat exchange area of heat exchanger varying with the natural gas flow

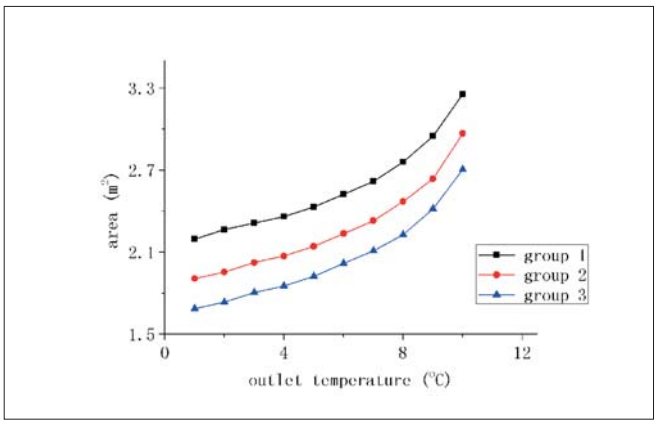

Fig. 7. Heat exchange area of the heat exchanger varying with the outlet temperature

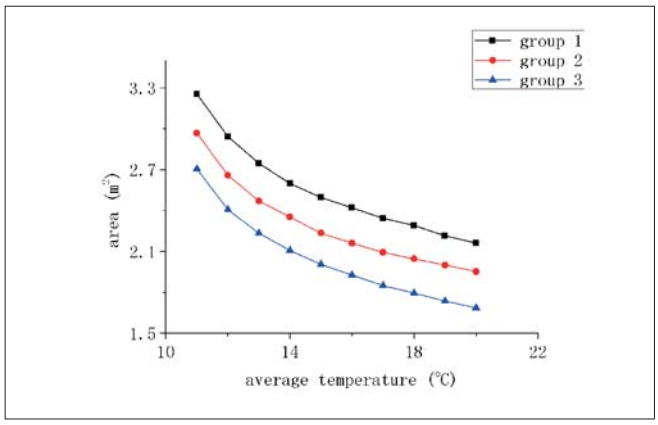

Fig. 8. Heat exchange area of heat exchanger varying with the temperature of the ethylene glycol solution

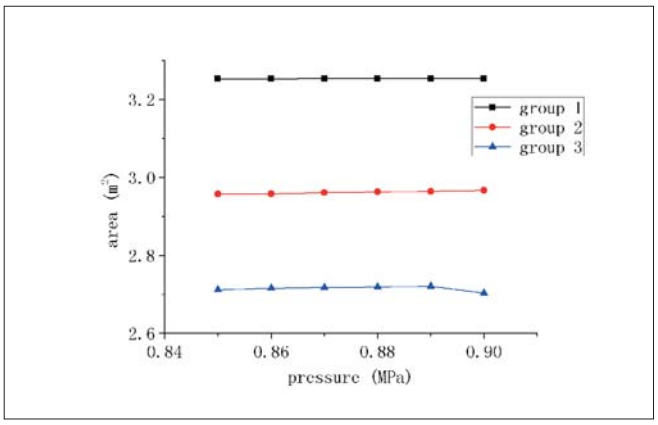

Fig. 9. Heat exchange area of heat exchanger varying with natural gas pressure

temperature of the spiral- wound heat exchanger must be maintained within a certain range. As the outlet temperature of the heat exchanger changes, the heat exchange area of the spiral-wound heat exchanger changes as shown in Fig. 7.

As shown in Fig. 7, the heat exchange area increases with the increase of the outlet temperature of the heat exchanger. Because the higher outlet temperature needs more heat exchange, increasing the heat exchange area can increase the heat exchange per unit of time. In addition, with the increase of the outlet temperature, the heat exchange area of the heat exchanger increases sharply. This is because, with the small temperature difference between hot and cold fluids at the end section of the heat exchanger, resulting in the reduction of heat flow per unit area, the heat exchange area required by natural gas to absorb the same amount of heat is larger than the first section of the heat exchanger.

The heat source for heating natural gas is ethylene glycol aqueous solution. Different temperatures of the ethylene glycol solution need a different heat exchange area of the spiral-wound heat exchanger to ensure that the temperature of the natural gas is at a certain value. It can be seen from the experiment that the temperature difference between the inlet and outlet of the ethylene glycol aqueous solution is small (about 2°C). Therefore, the change of temperature is reflected by the change of the average value of the inlet and outlet temperature. Under the premise that the outlet temperature of natural gas is 10°C, the relationship between the heat exchange area of the spiral-wound heat exchanger and the temperature of the ethylene glycol aqueous solution is shown in Fig. 8.

As shown in Fig. 8, the heat exchange area decreases with the increase of temperature of the ethylene glycol aqueous solution. This is because the temperature of the ethylene glycol solution increases and the temperature difference between hot and cold fluids increases, which leads to the increase of heat flow per unit area. When the same amount of heat is transferred, the larger the heat flow per unit area, the smaller the heat exchange area is required.

In order to study whether the heat exchange area is affected by the natural gas pressure, the relationship between the heat exchange area of the spiral-wound heat exchanger and the natural gas pressure is shown in Fig. 9.

As shown in Fig. 9, the heat exchange area hardly changes with the change of natural gas pressure. This is because the change of natural gas pressure has little influence on the parameters that affect the heat exchange area. Take pure methane as an example: when the pressure of pure methane decreases from 0.9 MPa to 0.85 MPa and the temperature remains at –100°C, the specific heat capacity will decrease by 0.93%, the density will decrease by 6.13%, the dynamic viscosity will decrease by 0.11%, and the thermal conductivity will decrease by 0.48%.

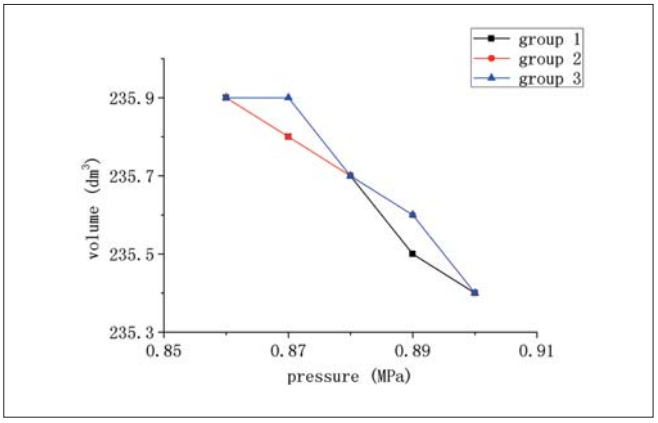

Fig. 10. Buffer tank volume varying with natural gas pressure

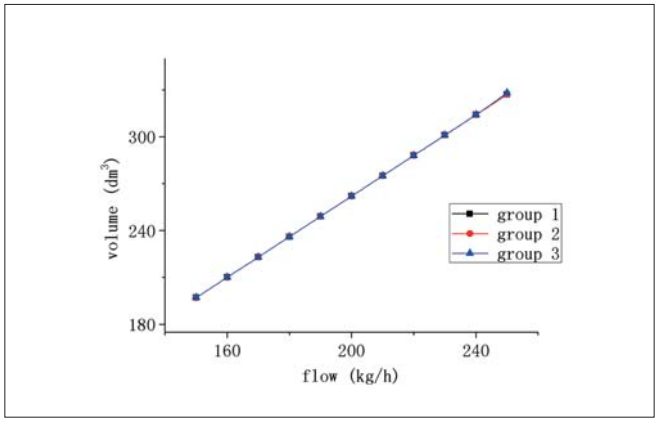

Fig. 11. Buffer tank volume varying with the natural gas flow

During the running process, the pressure of the natural gas will gradually drop. The variation of the buffer tank volume with the natural gas pressure is shown in Fig. 10.

As shown in Fig. 10, the volume of the buffer tank hardly decreases with the increase of the natural gas pressure. This is because the main factor influencing the buffer tank volume is the difference between the inlet and outlet natural gas flow. According to the van der Waals equation, pressure has little effect on mass. Therefore, when the natural gas pressure changes, the volume of the buffer tank changes very little. In addition, the buffer tank volume required for group 3 is larger than for group 1 and group 2. The buffer tank volume should be designed based on natural gas with a low methane content.

The natural gas flow of a dual fuel engine is different under different load conditions. The buffer tank needs to be adapted to sudden changes in natural gas flow. The variation of the buffer tank volume with natural gas flow is shown in Fig. 11.

As shown in Fig. 11, the buffer tank volume increases with increase of the natural gas flow. Due to the increase of the natural gas flow, the difference between the inlet and outlet flow increases, and a larger volume of buffer tank is needed to solve natural gas flow changes. In addition, the three groups of natural gas require the same buffer tank volume at different natural gas flows. The design of the buffer tank should consider the case of the maximum natural gas flow to avoid the shutdown of the dual fuel engine caused by the natural gas flow increasing suddenly.

CONCLUSION

A low-pressure gas supply system is designed for a dual fuel engine and experiments were conducted on it. The experimental data show that the system can supply gas stably during the start-up and running of the dual fuel engine, and that the dual fuel engine can run stably under various loads.

When designing the heat exchange area of the spiral-wound heat exchanger in the low-pressure gas supply system, the case of pure methane should be taken into account, so the calculated heat exchange area will also apply to natural gas with a low methane content. A larger heat exchange area is required when increasing the natural gas flow, increasing the outlet temperature of the natural gas and decreasing the temperature of the ethylene glycol solution. Although the heat exchange area has little relation with the natural gas pressure, the maximum natural gas pressure should be considered when calculating the heat exchange area. The volume of the buffer tank should increase with the increase of the natural gas flow. In addition, the volume of the buffer tank should be determined according to the minimum methane content.

ACKNOWLEDGEMENTS

The authors would like to acknowledge the support for the research provided by the National Natural Science Foundation of China (61403250).

REFERENCES

1. Yang Z. Y., Tan Q. M., Geng P. (2019): *Combustion and emissions investigation on low-speed two-stroke marine diesel engine with low sulfur diesel fuel*. Polish Maritime Research, 26, 153–161.

2. Wang Z. S., Lv J. G., Tan Y. F., Guo M., Gu Y. Y., Xu S., Zhou Y. H. (2019): *Temporospatial variations and Spearman correlation analysis of ozone concentrations to nitrogen dioxide, sulfur dioxide, particulate matters and carbon monoxide in ambient air, China*. Atmospheric Pollution Research, 10, 1203–1210.

3. Ray S., Kim K.-H. (2014): *The pollution status of sulfur dioxide in major urban areas of Korea between 1989 and 2010*. Atmospheric Research, 147-148, 101–110.

4. Lee S. B., Bae G. N., Lee Y. M., Moon K. C., Choi M. S. (2010): *Correlation between light intensity and ozone formation for photochemical smog in urban air of Seoul*. Aerosol and Air Quality Research, 10(6), 540–549.

5. Merien-Paul R. H., Enshaei H., Jayasinghe S. G. (2019): *Effects of fuel-specific energy and operational demands on cost/emission estimates: A case study on heavy fuel-oil vs liquefied natural gas*. Transportation Research Part D: Transport and Environment, 69, 77–89.

6. Yang Z. L., Zhang D., Caglayan O., Jenkinson I. D., Bonsall S., Wang J., Huang M., Yan X. P. (2012): *Selection of techniques for reducing shipping NOx and SOx emissions*. Transportation Research Part D: Transport and Environment, 17(6), 478–486.

7. Thomson H., Corbett J. J., Winebrake J. J. (2015): *Natural gas as a marine fuel*. Energy Policy, 87, 153–167.

8. Stoumpos S., Theotokatos G., Boulougouris E., Vassalos D., Lazakis I., Livanos G. (2019): *Marine dual fuel engine modelling and parametric investigation of engine settings effect on performance-emissions trade-offs*. Ocean Engineering, 157, 376–386.

9. Park H. J., Park, Lee S., Jeong J. Y., Chang D. J. (2018): *Design of the compressor- assisted LNG fuel gas supply system*. Energy, 158, 1017–1027.

10. Chien N. B., Jong-Taek O., Asano H., Tomiyama Y. (2019): *Investigation of experiment and simulation of a plate heat exchanger*. Energy Procedia, 158, 5635–5640.

11. Feng H. J., Chen L., Wu Z. X., Xie Z. J. (2019): *Constructal design of a shell-and-tube heat exchanger for organic fluid evaporation process*. International Journal of Heat and Mass Transfer, 131, 750–756.

12. Fang L., Diao N. R., Fang Z. H., Zhu K., Zhang W. K. (2017): *Study on the efficiency of single and double U-tube heat exchangers*. Procedia Engineering, 205, 4045–4051.

13. Fernández I. A. Gómez M. R., Gómez J. R., Insua A. B. (2017): *Review of propulsion systems on LNG carriers.* Renewable and Sustainable Energy Reviews, 67, 1395–1411.

14. Seo S. W., Jang W. H., Kim J. N. Y., Ryu J. H., Chang D. J. (2017): *Experimental study on heating type pressurization of liquid applicable to LNG fueled shipping*. Applied Thermal Engineering, 127, 837–845.

15. Wang W., Zhang Y. N., Lee K. S., Li B. X. (2019): *Optimal design of a double pipe heat exchanger based on the outward helically corrugated tube*. International Journal of Heat and Mass Transfer, 135, 706–716.

16. Wang G. H., Wang D. B., Peng X., Han L. L., Xiang S., Ma F. (2019): *Experimental and numerical study on heat transfer and flow characteristics in the shell side of helically coiled trilobal tube heat exchanger*. Applied Thermal Engineering, 149, 772–787.

17. Gupta P. K., Kush P. K., Tiwari A. (2007): *Design and optimization of coil finned-tube heat exchangers for cryogenic applications*. Cryogenics, 47, 322–332.

18. Saydam V., Parsazadeh M., Radeef M., Duan X.-L. (2019): *Design and experimental analysis of a helical coil phase change heat exchanger for thermal energy storage*. Journal of Energy Storage, 21, 9–17.

19. Abolmaali A. M., Afshin H. (2019): *Development of Nusselt number and friction factor correlations for the shell side of spiral-wound heat exchangers*. International Journal of Thermal Sciences, 139, 105–117.

20. Neeraas B. O., Fredheim A. O., Aunan B. (2017): *Experimental data and model for heat transfer, in liquid falling film flow on shell-side, for spiral-wound LNG heat exchanger*. International Journal of Heat and Mass Transfer, 47, 3565–3572.

21. Shah M. M. (1982): *Chart correlation for saturated boiling heat transfer: equations and further study*. ASHRAE Transactions, 88, 185–196.

22. Patil R. K., Shende B. W., Ghosh P. K. (1982): *Designing a helical-coil heat exchanger*. Chemical Engineering, 92, 85–88.

23. Wang Q. W., Zeng M., Ma T., Du X. P., Yang J. F. (2014): *Recent development and application of several high-efficiency surface heat exchangers for energy conversion and utilization*. Applied Energy, 135, 748–777.

CONTACT WITH THE AUTHORS

Xiaoyong Gu
e-mail: monkey9011@163.com
Shanghai Maritime University
1550 Haigang Avenue, 201306 Shanghai
China

Guohe Jiang
e-mail: ghjiang@shmtu.edu.cn
Shanghai Maritime University
1550 Haigang Avenue, 201306 Shanghai
China

Zhenghua Guo
e-mail: 15821421123@163.com
Shanghai Marine Equipment Research Institute
10 Hengshan Road , 200031 Shanghai
China

Shangzhi Ding
e-mail: 18688087651@163.com
Shanghai Marine Equipment Research Institute
10 Hengshan Road , 200031 Shanghai,
China